



HAL
open science

Chain Length Effect on the Structural and Emission Properties of the CuI/Bis((4-methoxyphenyl)thio)alkane Coordination Polymers

Adrien Schlachter, Rebecca Scheel, Daniel Fortin, Carsten Strohmann,
Michael Knorr, Pierre Harvey

► **To cite this version:**

Adrien Schlachter, Rebecca Scheel, Daniel Fortin, Carsten Strohmann, Michael Knorr, et al.. Chain Length Effect on the Structural and Emission Properties of the CuI/Bis((4-methoxyphenyl)thio)alkane Coordination Polymers. *Inorganic Chemistry*, 2022, 61 (29), pp.11306-11318. 10.1021/acs.inorgchem.2c01427 . hal-03762998

HAL Id: hal-03762998

<https://hal.science/hal-03762998v1>

Submitted on 12 Sep 2024

HAL is a multi-disciplinary open access archive for the deposit and dissemination of scientific research documents, whether they are published or not. The documents may come from teaching and research institutions in France or abroad, or from public or private research centers.

L'archive ouverte pluridisciplinaire **HAL**, est destinée au dépôt et à la diffusion de documents scientifiques de niveau recherche, publiés ou non, émanant des établissements d'enseignement et de recherche français ou étrangers, des laboratoires publics ou privés.

Chain Length Effect on the Structural and Emission Properties of the CuI/Bis((4-methoxyphenyl)thio)-alkane Coordination Polymers

Adrien Schlachter^{*,1} *Rebecca Scheel*^{,2} *Daniel Fortin*^{,1} *Carsten Strohmann*^{,2} *Michael Knorr*^{3*} and *Pierre D. Harvey*^{1*}

† Dedicated to the memory of our colleague and friend Kevin Tanner, deceased in 2022.

¹Département de Chimie, Université de Sherbrooke 2500 Boulevard Université, Sherbrooke, PQ, Canada, J1K 2R1.

²Anorganische Chemie, Technische Universität Dortmund, Otto-Hahn-Straße 6, 44227 Dortmund, Germany.

³Institut UTINAM, UMR CNRS 6213, Université Bourgogne Franche-Comté, 16, Route de Gray, 25030 Besançon, France.

KEYWORDS. Crystals, Luminescence, Ligands, Metal clusters, Physical and chemical processes.

ABSTRACT: A systematic chain length variation of the ligand $\text{MeOC}_6\text{H}_4\text{S}(\text{CH}_2)_m\text{SC}_6\text{H}_4\text{OMe}$ ($1 \leq m \leq 8$) was performed to study its effect on the structures and photophysical properties of the coordination polymers (CP) when reacted with CuI. Indeed, direct correlations are noted between these features and m . When m is an odd number, the secondary building unit is systematically the common closed cubane Cu_4I_4 cluster, rendering the material strongly luminescent (*i.e.* emission quantum yield, $\Phi_e > 20\%$), and the CP is 1D. However when m is 2, 4 and 6, the SBUs exhibit rare polymeric motifs of $(\text{Cu}_2\text{I}_2)_n$: staircase ribbon, fused poly(rhombic pseudo-dodecahedron) and accordion ribbon, respectively, and the emission intensities are either very weak ($\Phi_e < 0.001$

%) or of medium intensity ($\Phi_e \sim 10\%$ when $m = 6$). When $m = 8$ (*i.e.* the most flexible chain), the SBU is a closed cubane Cu_4I_4 and the emission intensity is medium ($\Phi_e \sim 10\%$). A special case was observed for $m = 3$, where a co-crystallization of the molecular cluster $\text{Cu}_4\text{I}_4(\text{NCCH}_3)_4$ is observed in the lattice, which turns out to be quite important for the stability of the network.

INTRODUCTION

Since the pioneer works by H. D. Hardt, E. Holdt in the late 70ies¹⁻⁴ and later by Peter Ford and his collaborators in the 80ies on neutral copper(I) halide clusters $\text{Cu}_x\text{X}_x\text{Ly}$ ($\text{X} = \text{I}; 2, 4, y = 4$),⁵ this chemistry has been extended to a larger family of $\text{Cu}_x\text{X}_x\text{Ly}$ -containing complexes and coordination polymers (CP; $\text{X} = \text{Cl, Br, I, OH}; 2 < x < 8, y = 4, \dots$).⁶⁻¹⁴ This field is largely dominated by N- and P-donor ligands and significant advances in the field of material science were made.¹⁵⁻²⁰ In particular, when $\text{X} = \text{I}$, the clusters, namely the closed cubane Cu_4I_4 , the resulting responsive materials turn out to be strongly emissive, and properties such as vapo-, solvato-, mechano- and thermochromism have been reported.^{12,19,21-29} The effect of the aliphatic chain length variation chain that connects two $\text{N}\equiv\text{C}/\text{P}$ -donor units with ditopic linkers on the outcomes of their coordination chemistry on coinage metal ions was also previously studied.³⁰⁻³⁵

Concurrently, chalcogenoether and chalcogenide ligands also form an important class of 1D-, 2D- and 3D-CPs when reacted with copper(I) halides.³⁶ Indeed, these networks also exhibit rich properties such as solid-to-solid phase transition, vapo-, solvato- and thermochromism, photo- and electroluminescence, redox activity, (semi)conductivity, porosity, gas adsorption, cytotoxicity and antibacterial behaviors leading to applications such as solar cells, light emitting diodes, heterogeneous catalysis and photocatalysis, stimuli-responsive smart and self-healing materials, sensors and cancer therapy.³⁷ These CPs are constructed with neutral $(\text{CuX})_n$ clusters ($\text{X} = \text{Cl, Br, I}$), often referred as secondary bonding units (SBUs), where $1 \leq n \leq 8$ or more rarely $n = \infty$ (1D-SBU), and mono- or polychalcogene-containing ligands. Both entities define the resulting network properties. The SBU motifs can be separated into two large categories: *quasi-planar* and *globular* clusters dominated by respectively the rhomboid and closed cubane (when $\text{X} = \text{I}$) motifs (Figure 1). One key difference is that when *globular* SBUs are formed, the CPs are found strongly emissive (*i.e.* $\Phi_e \geq 10\%$),³⁶ and when *quasi-planar* SBUs are generated, the isolated network is found weakly or not emissive.³⁶ One exception was recently reported for a 3D-CP $[(\text{Cu}_8\text{I}_8)(\text{L4})_2]_n$

(CP4) formed when CuI was reacted with *para*-MeOC₆H₄S(CH₂)₄SC₆H₄OMe (**L4**) in which an very rare 1D-SBU (Cu₈I₈)_n as a poly(truncated rhombic dodecahedron), formed.³⁸ Concurrently when *m* = 1, a strongly emissive 1D-CP of formula [Cu₄I₄(ligand)₂]_n (**CP1**) formed instead where the SBU is a closed cubane.^{39,40} This observation suggests that the CP structure and SBU motif, and consequently, the network's properties, appear to be chain length dependent. This hypothesis is reinforced by examining the CPs formed during the reaction between CuI and the *para*-MeC₆H₄S(CH₂)_{*m*}SC₆H₄Me ligand: *m* = 1, 1D-CP, SBU = Cu₄I₄,⁴⁰ *m* = 5, 1D-CP, SBU = Cu₄I₄,⁴⁰ *m* = 8, 2D-CP, SBU = fused dicubane Cu₈I₈,⁴¹ thus suggesting that an odd number of carbons in the flexible (CH₂)_{*m*} chain is rather prone to form emissive 1D-CPs with closed cubane Cu₄I₄ SBUs, whereas an even number is prone to form other types of CPs.

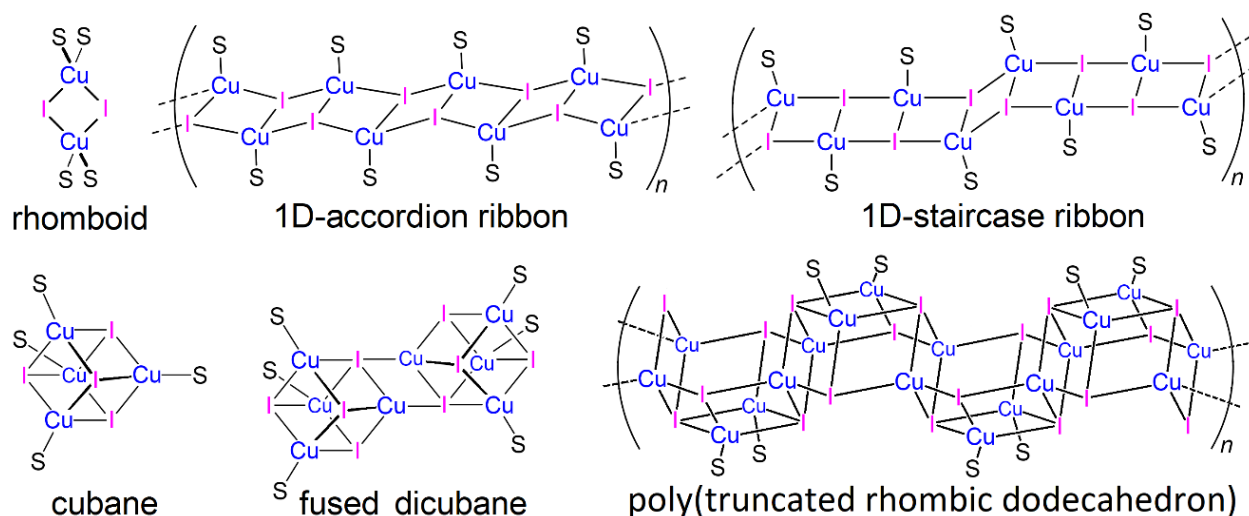


Figure 1. Structures of three selected *quasi-planar* SBUs (top) and three *globular* SBUs (bottom) for CPs formed during the reaction between CuI and thioethers. This list is not exhaustive.³⁶

Since the CP and SBU structures, and thus their properties, are linked to the number of carbons in the chain, a systematic study appears necessary as the sampling appears meager and heterogenous. We now report the synthesis and characterization of six CPs formed during the reaction between CuI and the *para*-MeOC₆H₄S(CH₂)_{*m*}SC₆H₄OMe ligands (**Lm**; *m* = 2, 3, 5-8) where *m* = 2 (**CP2**), 3 (**CP3**), 5 (**CP5**), 6 (**CP6**), 7 (**CP7**) and 8 (**CP8**), thus completing a series going from *m* = 1 to 8. Clear trends relating the CP dimensionality, SBU motif, and resulting emission properties depending whether odd and even numbers of carbons form the (CH₂)_{*m*} central chain, and the effect of grinding and exposing to various solvent when pertinent, are noted.

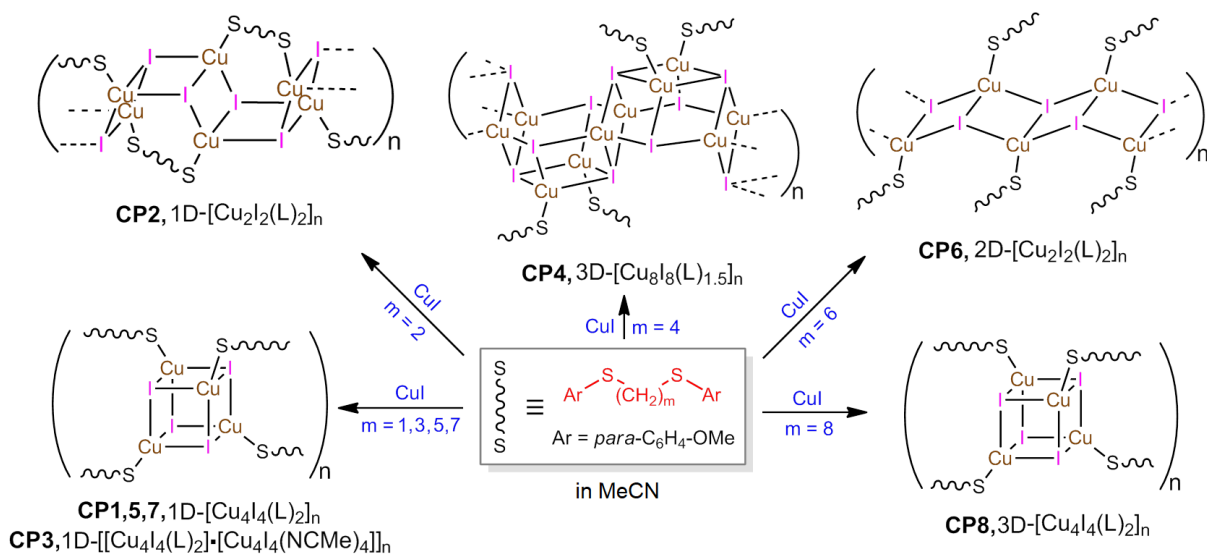
RESULTS AND DISCUSSION

General. The syntheses of **CP1-CP8** are summarized in Scheme 1. They consist at reacting CuI with the corresponding **L1-L8** ($\text{ArS}(\text{CH}_2)_m\text{SAr}$; $\text{Ar} = \textit{para}\text{-C}_6\text{H}_4\text{OMe}$; $m = 1\text{-}8$) in acetonitrile (or in some case in EtCN) in a 1:2 stoichiometric ratio. All polymers were characterized by IR, Raman (Figures S1 and S2), TGA (Figure S3), powder X-ray diffraction patterns (XRD), and elemental analysis. Their identity was confirmed by X-ray crystallography and modeling for **CP7** (Table 1, Table S1-S3).

Table 1. List of CPs investigated in this work.^{a,b,c}

CP (<i>T</i> , <i>K</i>)	SBU	formula	Shortest distance Cu...Cu (Å)	Mean distance Cu...Cu (Å)
CP1 ^{39,40} (130)	cubane	1D-[Cu ₄ I ₄ (L1) ₂] _n	2.625(5)	2.702
CP2 (123)	curtain wall	1D-[(Cu ₂ I ₂)(L2)] _n	2.8662(7)	2.872
CP3 (173)	cubane	1D- [{Cu ₄ I ₄ (L3) ₂ } _{3.5} •Cu ₄ I ₄ (MeCN) ₄ •4MeCN] _n	2.691(3) ^a 2.694(3) ^b	2.707 ^a 2.783 ^b
CP3' (173)	rhomboid	1D-[{Cu ₂ I ₂ (L3) ₂ }•EtCN] _n	2.8833(10) ^c 2.8764(9) ^d	2.880
CP4 ³⁸ (100)	<i>e</i>	3D-[Cu ₈ I ₈ (L4) _{1.5}] _n	2.7910(2)	2.908
CP5 (173)	cubane	1D-[Cu ₄ I ₄ (L5) ₂] _n	2.7315(18)	2.810
CP6 (173)	accordion	2D-[(Cu ₂ I ₂)(L6)] _n	2.7571(11)	3.138
CP7 (173)	Cubane ^f	1D-[Cu ₄ I ₄ (L7) ₂] _n ^f	2.50 ^f	2.95 ^f
CP8 (100)	cubane	3D-[Cu ₄ I ₄ (L8) ₂] _n	2.6942(3)	2.768

^{a,b}There are two types of closed cubane clusters inside the materials: a = Cu₄I₄(NCMe)₄. b = Cu₄I₄S₄, ^c Ribbon A (see Figure S4), ^d Ribbon B (see Figure S4), ^eSBU = poly(truncated rhombic dodecahedron), see Figure 1. ^fThe structure was solved by computer modeling based on the PXRD data (detail below).



Scheme 1. Reaction schemes for the syntheses of **CP1-CP8**. Note that **CP3** bears four MeCN crystallization molecules and **CP1** and **CP4** have been previously reported by us and are listed for comparison purposes.³⁸⁻⁴⁰

The CPs are thermally stable up to temperatures approaching or 200°C according to TGA data (Table 2, the traces and first derivatives are in Figure S3). The exception is **CP3**, which contains four acetonitrile as crystallization molecules and four coordinated ones. This weight loss occurs at 86°C which is not too different from its boiling point ($T_{\text{boiling}}(\text{MeCN}) = 82^\circ\text{C}$). **CP3** also exhibit the lowest temperature of decomposition. Speculatively, the weight loss may be associated with the presence of coordinated acetonitrile molecules (see structure below).

Table 2. TGA data for **CP2**, **CP3**, **CP3'**, **CP5**, **CP6**, **CP7**, and **CP8** under argon.

	Formula [M (g.mol ⁻¹)] ^a	T_{Dec} (°C) ^b	$\text{Exp } \Delta m$ (%)	$\text{Calc } \Delta m$ (%)	Attribution
CP2	C ₁₆ H ₁₈ Cu ₂ I ₂ O ₂ S ₂ [687.30]	210 548	-43.42 -44.44	-44.58 -43.86	L2 2 I + 0.75 Cu
CP3	C ₁₁₈ H ₁₄₄ Cu ₁₄ I ₁₄ N ₈ O ₁₂ S ₁₂ [4917.28] ^c	86 191 450	-7.26 -39.39 -33.71	-6.68 -39.10 -33.55	8 MeCN 6 L3 13 I
CP3'	C ₃₇ H ₄₅ Cu ₂ I ₂ NO ₄ S ₄ [1076.86]	87 261 557	-4.67 -56.78 -29.92	-5.11 -59.52 -29.47	EtCN 2 L3 2 I + Cu
CP5	C ₁₉ H ₂₄ Cu ₂ I ₂ O ₂ S ₂ [729.38]	235 635	-57.80 -33.39	-56.48 -34.81	L5 + 0.5 I 1.5 I + Cu
CP6	C ₁₀ H ₁₃ CuIOS [371.70]	227	-49.26	-48.77	0.5 L6

		618	-40.22	-39.27	I + 0.3 Cu
CP7	C ₂₁ H ₂₈ Cu ₂ I ₂ O ₂ S ₂ ^a [757.47]	246	-50.27	-49.71	L7
		593	-41.60	-41.89	2 I + Cu
CP8	C ₁₁ H ₁₅ CuIOS [385.73]	256	-50.60	-50.63	0.5 L8
		602	-38.30	-37.02	I + 0.25 Cu

^a Formula and molecular mass for one repetitive unit. ^b Reported at the temperature where the CP loses weight. ^c **CP3** starts exhibiting weight loss near room temperature until the large weight loss at 191°C. This gradual weight loss is most likely due to the Cu₄I₄(NCMe)₄ decomposition.

X-ray structure of **CP2** (1D-[(Cu₂I₂)(**L2**)_n]). In contrast to the reaction of PhSCH₂CH₂SPh with CuI (ratio metal/ligand 2:1) yielding a 2D material [(CuI)₂{μ-PhS(CH₂)₂SPh}₂]_n incorporating rhomboid-shaped Cu(μ₂-I)₂Cu SBUs, the X-ray determination of **CP2** revealed a profound change of both the dimensionality and nuclearity. Figure 2 shows that 1D-ribbons have been formed where the (CuI)_n chain adopts a curtain wall structure (two views of crystal packing are provided in Figure S5). This rare, folded motif is induced by the small bite separation of **L2** (d(S⋯S) = 4.400 Å), which is acting as a bridging ligand between two Cu(I) on the same face of the ribbon making -CH₂S-Cu-I-Cu-I-Cu-SCH₂-rings. The bridged Cu⋯Cu separation is 5.561 Å. Some ring stress is also noted when comparing the shortest d(Cu⋯Cu) distance in **CP2** (2.8662(7) Å) with shortest ones measured for the other CPs (from 2.625(5) to 2.7910(2) Å) falling in this same category of MeOC₆H₄-containing ligands (**CP1-CP8**; Table 1). For **CP2**, this distance is the longest. Based on a recent review, this motif is quite unique in chalcogenoether-containing network.³⁶ The only other examples for 1D-(CuI)_n ribbons featuring SBU of this type with μ₃-linking iodide atoms are the 1D-staircase ribbon in [{Cu(μ₃-I)₂Cu}(μ-ferrocenyldithiane)]_n (mean d(Cu⋯Cu) = 2.7384 Å; Figure 3)⁴² and the 1D-[(Cu₂I₂)(*para*-MeC₆H₄SCH₂CH₂SC₆H₄Me)₂]_n CP (d(S⋯S) = 4.444 Å; bridged d(Cu⋯Cu) = 5.569 Å; shortest d(Cu⋯Cu) = 2.907 Å).⁴³

The resemblance of this latter bis(4-tolylthio)ethane ligand with **L2** is striking meaning that the change of the methoxy group by a methyl substituent impacts only little the outcome of the SBU motif and CP dimensionality. However, when the dithioether ligand is either R = H³⁹ or Cl⁴⁴, quasi-identical honeycomb-like 2D-CPs are obtained. This variation in SBU motif and CP dimensionality is consistent with what is expected when comparing an H-atom and a Me group substituted at the *para*-position of benzene. Indeed for RC₆H₄S(CH₂)₈SC₆H₄R, when R = H and Me, the reactions with CuI respectively lead to the CPs 1D-[Cu₄I₄(**L**)₂]_n and 2D-[Cu₈I₈(**L**)₃]_n where Cu₄I₄ is a closed cubane and Cu₈I₈ is a fused closed dicubane motif.⁴⁵

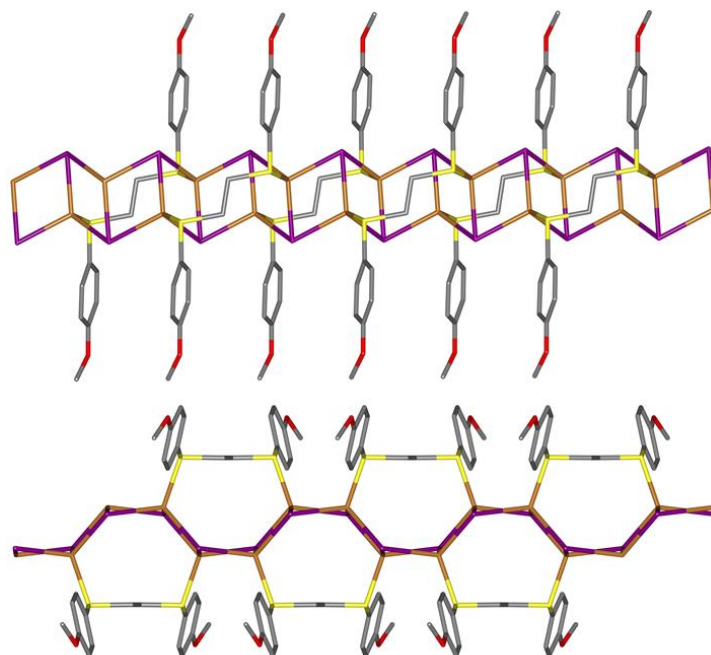


Figure 2. Structure of the 1D-curtain wall ribbon of **CP2**. Top: top view. Bottom: side view. Color code: brown (Cu), purple (I), yellow (sulfur), red (oxygen), grey (carbon). The H-atoms are not shown for clarity.

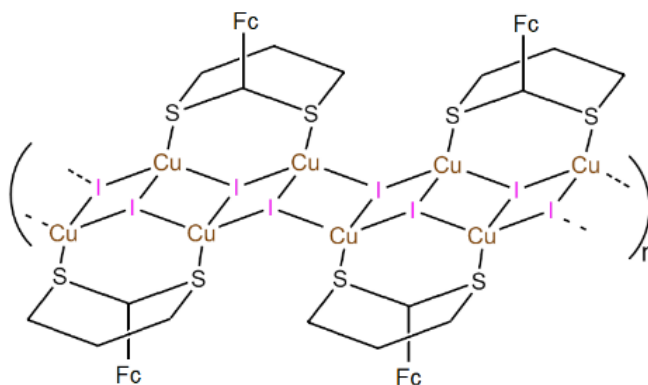


Figure 3. Structure of the 1D-staircase ribbon $[\{\text{Cu}(\text{m}_3\text{-I})_2\text{Cu}\}(\mu\text{-ferrocenyldithiane})]_n$.⁴²

The X-ray structure of **CP2** was also examined at various temperatures (123, 173, 223 and 298 K; the X-ray parameters are placed in Table S1). No phase change was noted for which the space group remains $C 2/c$. The unit cell parameters a , b , c , and the volume (V) increase only slightly with the temperature (Table 1; Figure S6), except for the a axis, which undergoes a slight

decrease between 173 and 223 K. The Cu···Cu separations also increase slightly (by $\sim 0.035\text{\AA}$ on average) going from 123 to 298 K).

X-ray structure of **CP3** ($1\text{D}-[\{\text{Cu}_4\text{I}_4(\text{L3})_2\}_{3.5}\cdot\text{Cu}_4\text{I}_4(\text{MeCN})_4\cdot 4\text{MeCN}]_n$). **CP3** was obtained by reacting $\text{MeOC}_6\text{H}_4\text{S}(\text{CH}_2)_3\text{SC}_6\text{H}_4\text{OMe}$ with CuI in MeCN with metal/ligand ratios of 1:1, 1:1.5, and 2:1. The crystal structure of **CP3** is unique among the chalcogenoether/copper halide-based networks³⁶ as it exhibits a lattice containing two different co-crystallized CuI-containing species. It includes a $1\text{D}-[\text{Cu}_4\text{I}_4(\text{L3})_2]_n$ chain, which resembles that of the $1\text{D}-[\text{Cu}_4\text{I}_4(\text{L1})_2]_n$ CP,^{39,40} and a discrete closed cubane $\text{Cu}_4\text{I}_4(\text{NCMe})_4$ (Figure 4a,b). The X-ray structure of the $\text{Cu}_4\text{I}_4(\text{NCMe})_4$ cluster has previously been reported and coincidentally this cluster too co-crystallizes with a second molecule (dibenzo-18-crown-6 in the other case).⁴⁶ The bond lengths and angles of $\text{Cu}_4\text{I}_4(\text{NCMe})_4$ in **CP3** are fully consistent with those reported earlier suggesting that the cubane structure is not significantly affected by the crystal packing. The $\text{Cu}_4\text{I}_4(\text{NCMe})_4$ cubanes (in blue in Figure 4c,d) are located inside quasi-square-shaped channels formed by eight $1\text{D}-[\text{Cu}_4\text{I}_4(\text{L3})_2]_n$ columns. These channels are formed by four piled-up sides composed of the planar $\text{C}_6\text{H}_4\text{OMe}$ groups piling in a slipped manner (Figure S7). **CP3** remains stable under standard conditions several weeks prior to deteriorate (see Figure S8). The crystals of **CP3** turn opaque over a few days without any spectral changes in the PXRD patterns. Because of the formation of channels within the lattice, one wonders whether the MeCN crystallisation molecules and/or $\text{Cu}_4\text{I}_4(\text{NCMe})_4$ could be exchanged or removed when exposed to solvents known to be poor solvents for **CP3** (Figure S8). Stability test was first performed as a control experiment upon comparing the PXRD patterns of a fresh solid sample and the same sample left in air for several weeks (Control). A small deterioration of the PRXD pattern was observed but the spectral structure remained intact. Upon leaving **CP3** exposed to acetonitrile, the PXRD signature remained identical as the fresh sample as expected. However, when exposed to benzene and toluene, both PXRD responses are the same but change drastically indicating a crystal transformation. Incidentally, the resulting signature is clearly reminiscent to that obtained for $1\text{D}-[\text{Cu}_4\text{I}_4(\text{L5})_2]_n$ below, which strongly suggest isostructurality and consequently meaning that the $\text{Cu}_4\text{I}_4(\text{NCMe})_4$ has successfully been extracted from the lattice. Unfortunately, attempts to obtain crystals suitable for X-ray analysis stubbornly failed. Nevertheless, this experiment turns out to be useful for assigning the most emissive species: ($\text{Cu}_4\text{I}_4(\text{NCMe})_4$ versus $1\text{D}-[\text{Cu}_4\text{I}_4(\text{L3})_2]_n$),

which is addressed in a section below. When **CP3** is exposed to CH_2Cl_2 and xylene, the resulting PXRD pattern is identical to that for $\gamma\text{-CuI}$, which indicates decomposition.

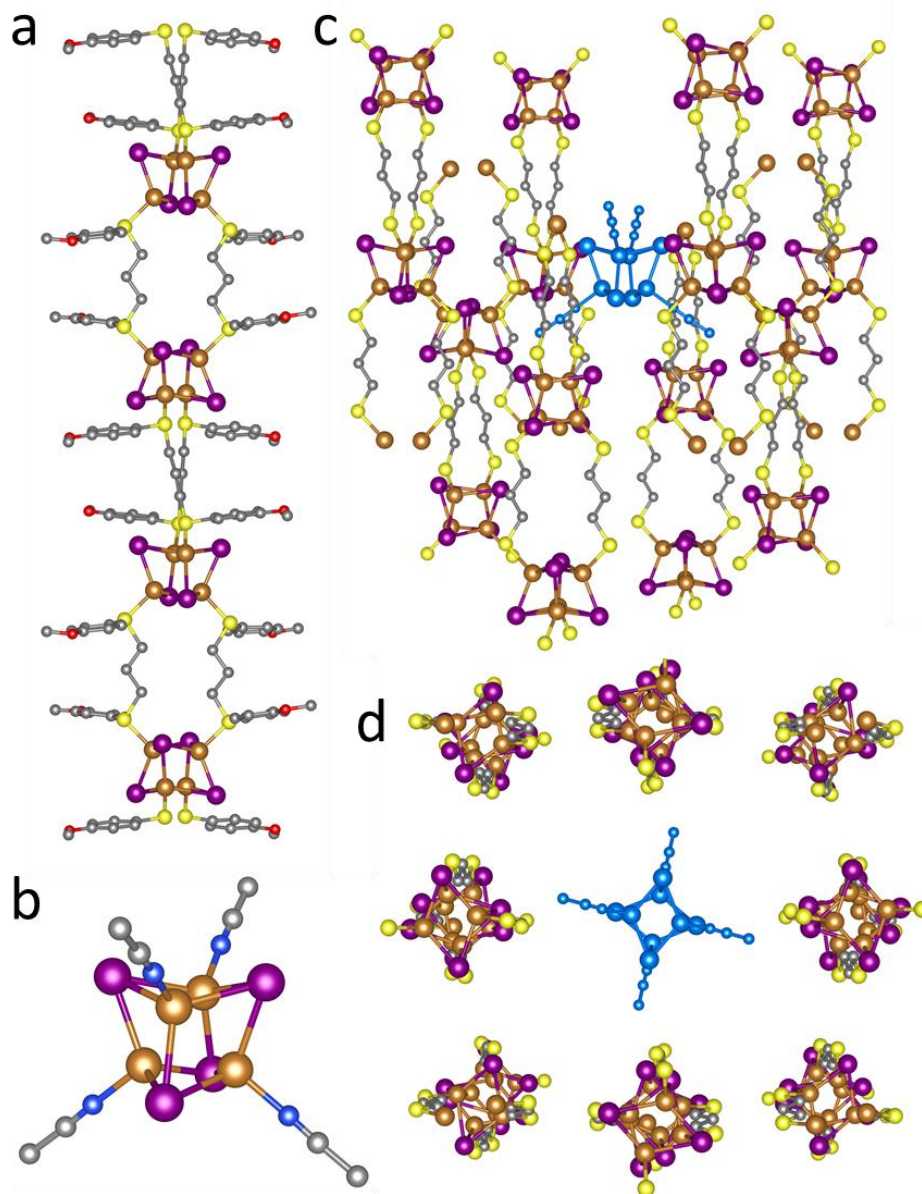


Figure 4. (a) X-ray structure of the 1D- $\{\text{Cu}_4\text{I}_4(\text{L3})_2\}_{3.5}$ -chain. (b) Structure of $\text{Cu}_4\text{I}_4(\text{NCMe})_4$. The H-atoms and crystallization acetonitrile molecules are not shown for clarity in a and b. (c) (d) Side and top views of the relative position of the $\text{Cu}_4\text{I}_4(\text{NCMe})_4$ cluster (in blue) in the lattice. The $\text{C}_6\text{H}_4\text{OMe}$ groups are not shown for clarity. Color code: brown (Cu), purple (I), yellow (sulfur), red (oxygen), grey (carbon), blue (nitrogen and central $\text{Cu}_4\text{I}_4(\text{NCMe})_4$).

Moreover, because the $\text{Cu}_4\text{I}_4(\text{NCMe})_4$ cluster occupies a given space, then changing MeCN for EtCN should prevent the anticipated analogous cluster ($\text{Cu}_4\text{I}_4(\text{NCeT})_4$) to enter the lattice, or even form. Indeed, by exposing **CP3** to EtCN at room temperature for several days, new crystals form. The X-ray data reveals the presence of a 1D-CP of formula $1\text{D}-[\text{Cu}_2\text{I}_2(\text{L3})_2 \cdot \text{EtCN}]_n$ (**CP3'**) where EtCN is a crystallisation molecule and the SBU is a rhomboid with no evidence of the $\text{Cu}_4\text{I}_4(\text{NCMe})_4$ cluster or Cu_4I_4 cubane in the polymeric chain (Figure 5 and S7). The **CP3'** structure is reminiscent of that of the 1D-CPs $[\text{Cu}_2\text{Br}_2(\text{PhS}(\text{CH}_2)_3\text{SPh})_2]_n$ ⁴⁷ and $[\text{Cu}_2\text{I}_2(\text{p-FC}_6\text{H}_4\text{S}(\text{CH}_2)_3\text{S-p-C}_6\text{H}_4\text{F})_2]_n$ ⁴⁸ There are two independent parallel chains in the unit cell (Figure S9). Their Cu_2I_2 rhomboids exhibit $\text{Cu}\cdots\text{Cu}$ separations of 2.883 and 2.876 Å, both slightly above the van de Waals radii of two Cu atoms (2.8 Å). The absence of any Cu_4I_4 cluster in **CP3'** is indicative that the $\text{Cu}_4\text{I}_4(\text{NCMe})_4$ cluster in **CP3** has a stabilizing effect of the lattice. In conclusion, the lattice structure of **CP3** is found to be rather unique but also somewhat fragile thermally (based on the TGA traces, **CP3** exhibits the lowest T_{dec} as weight loss starts appearing soon after room temperature; Figure S10) or when exposed to given solvents. By comparison, **CP3'** losses EtCN in the vicinity of 100 °C (Figure S10).

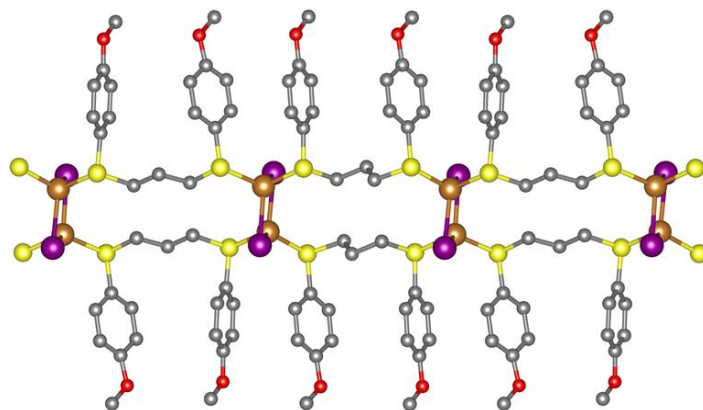


Figure 5. X-ray structure of **CP3'** ($1\text{D}-[\{\text{Cu}_2\text{I}_2(\text{L3})_2\} \cdot \text{EtCN}]_n$). The H-atoms and EtCN molecules are not shown for clarity. Color code: brown (Cu), purple (I), yellow (sulfur), red (oxygen), grey (carbon).

X-ray structure of **CP5** $1\text{D}-[\text{Cu}_4\text{I}_4(\text{L5})_2]_n$. **CP5** was obtained by reaction of CuI with the ligand $\text{MeOC}_6\text{H}_4\text{S}(\text{CH}_2)_5\text{SC}_6\text{H}_4\text{OMe}$ **L5** in a 2:1 ratio and crystallizes in a 1D-ladder structure where step-shaped macrocycles of $[(\text{Cu}_4\text{I}_4)_2(\text{L5})_2]_2$ dimers are linked to other dimers by two μ_2 -**L5** ligands to form a CP better described as $\{[(\text{Cu}_4\text{I}_4)_2(\text{L5})_2]_2(\mu_2\text{-L5})_2\}_n$ (Figure 6). It is noteworthy

that this ladder-shaped 1D CP motif appears unique in chalcogenoether-containing materials.³⁶ The nodes are closed cubanes Cu_4I_4 where all Cu-centers are coordinated to one S-atom of four different ligands. This structure differs from what is reported for ligands containing ArSCH_2SAr (Ar = aromatic group) for obvious steric reasons of the short methylene chain.⁴⁰ This steric restriction is also noted for $\text{PhS}(\text{CH}_2)_3\text{SPh}$, which form a 2D-sheet $[\text{Cu}_4\text{I}_4(\text{PhS}(\text{CH}_2)_3\text{SPh})_2]_n$ instead.⁴⁷ However, when the ligand is $\text{PhS}(\text{CH}_2)_5\text{SPh}$, the dimensionality of this CP is also 1D with closed cubane Cu_4I_4 SBUs but no $[(\text{Cu}_4\text{I}_4)_2(\text{PhS}(\text{CH}_2)_3\text{SPh})_2]_2$ macrocycles is formed.⁴⁷ This observation implies that the OMe group plays a significant role on this outcome. It is noteworthy that **CP1** exhibits two symmetry-related crystallographically different Cu atoms and that the core motif of **CP3** and **CP5** contains four crystallographically different Cu(I) centers (Figure 7). In contrast, the highly symmetric cluster core of **CP8** (see below) bears four identical CuI units.

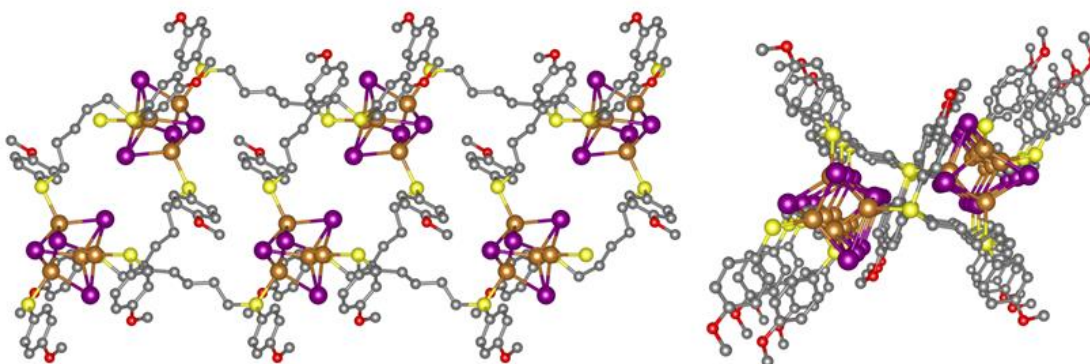


Figure 6. X-ray structure of **CP5** ($1\text{D}-[\text{Cu}_4\text{I}_4(\text{L5})_2]_n$). Side view (left) and view along the 1D-propagation (right). The H-atoms are not shown for clarity. Color code: brown (Cu), purple (I), yellow (sulfur), red (oxygen), grey (carbon).

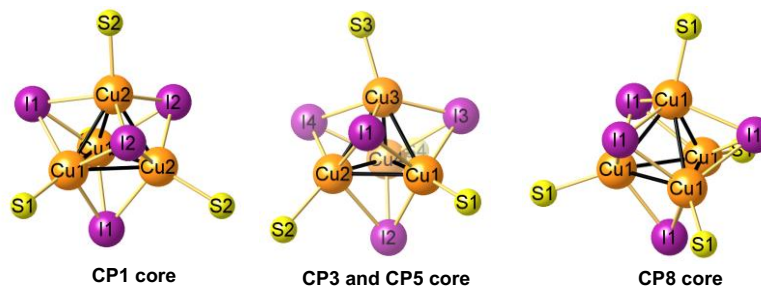


Figure 7. Views of the cubane $\text{Cu}_4(\mu_3\text{-I})_4\text{S}_4$ cores within **CP1**, **CP3**, **CP5** and **CP8** featuring different symmetries.

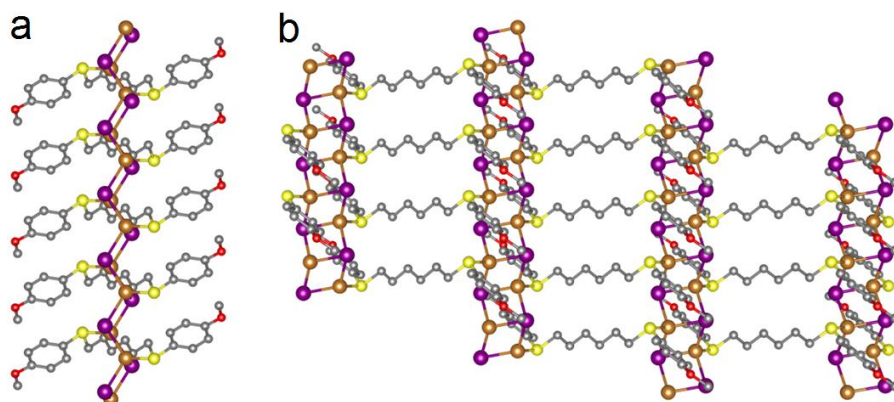


Figure 8. X-ray structure of **CP6** ($2D-[Cu_4I_4(L6)_2]_n$). (a) Side view of the $1D-(CuI)_n$ accordion ribbon (only part of **L6** is shown for clarity). (b) View of the 2D-organisation of **CP6**. The H-atoms are not shown for clarity. Color code: brown (Cu), purple (I), yellow (S), red (O), grey (C).

X-ray structure of **CP6** ($2D-[(Cu_2I_2)(L6)]_n$). This colorless and air stable material **CP6** was obtained by reaction of CuI with the ligand $MeOC_6H_4S(CH_2)_5SC_6H_4OMe$ **L6** (2:1 CuI-to ratio) in MeCN solution (Scheme 1) and crystallizes as 2D-sheets (Figure 8 and Figure S11). These layers are composed of accordion-shaped $1D-(CuI)_n$ ribbons, which are interlinked sideways by **L6** ligands. The ribbons contain crystallographically identical Cu atoms, which weakly interact with the neighbored one through a Cu-Cu contact of 2.7571(11) Å. Like in **CP2**, each Cu-Cu couple is linked to the adjacent ones through a μ_3 -bridging iodide atom. This 1D-accordion ribbon motif for the SBU is rare but not uncommon based on a recent survey.³⁶ This architecture contrasts with that observed for the related CP $1D-[(Cu_4I_4)(PhS(CH_2)_6SPh)]_n$, where the SBU is a closed cubane and the dimensionality is 1D.⁴³ This comparison is another example of a drastic difference when replacing an H-atom by a OMe substituent at the *para*-positions of **Lx**.

X-ray structure of **CP7** ($1D-[(Cu_4I_4)(L7)]_n$). No crystal of suitable quality for X-ray diffraction studies was obtained for this strongly emissive species. Instead, computer modeling and simulation of powder XRD pattern were employed to elucidate the structure. Based on a crystal structure collection enumerated in a review article dedicated to copper-halide chalcogenides networks, two main conclusions arise from it.³⁶ First, two main categories of SBUs exist, *globular* and *quasi-planar* (Figure 1), where the former shape is prone to rich luminescence properties, such as large emission quantum yields and long lifetimes, whereas the latter type is not.³⁶ The photophysical data for **CP7** are presented below and strongly suggest that the SBU of **CP7** belongs to the *globular* category. Second, statistics indicate that the 1D- (41%) and 2D- (39%)

CPs represent 80% of all Cu_4I_4 -containing networks.³⁶ Finally, **CP1**, **CP3** and **CP5** form 1D-CPs and are built with **L1**, **L3** and **L5**, respectively, with $(\text{CH}_2)_m$ chains where m is odd. These information orientate the primary modeling towards the highly probable 1D- $[(\text{Cu}_4\text{I}_4)(\text{L7})]_n$, the other being a 2D-version.

Views of the packing are provided in Figures S12 and S13. Figure S14 compares the simulated PXRD pattern of a calculated model (Figure 9; monoclinic system, $P2_1/n$ $P2$ space group; $a = 24.471 \text{ \AA}$, $b = 14.397 \text{ \AA}$, $c = 17.617 \text{ \AA}$, $\beta = 114.855^\circ$) with the experimental. A good agreement with experimental data with a percentage of similarity of 98.7% is observed after compensating for the baseline discrepancies ($R_{wp}(w/o \text{ bck})$). Moreover, the calculated filled and void spaces (using Crystal Maker) for this model fall in the middle of the range of filled and void spaces of the other crystals investigated in this work (Table S4). Other calculated structures based on common X-ray data throughout the literature were also investigated,³⁶ but the comparison between the experimental and simulated data were poor. All in all, this 1D-motif turned to be the best. Moreover, the calculated Cu-Cu distances inside the Cu_4I_4 cluster were evaluated based on the refined structure and ranges from 2.5 up to 3.0 \AA with an average of $\sim 2.7 \text{ \AA}$. This value falls perfectly within the distribution of Cu-Cu distances reported throughout the literature³⁶ thus reinforcing the predictable nature of the Cu-Cu distances in the Cu_4I_4 cubane motifs.

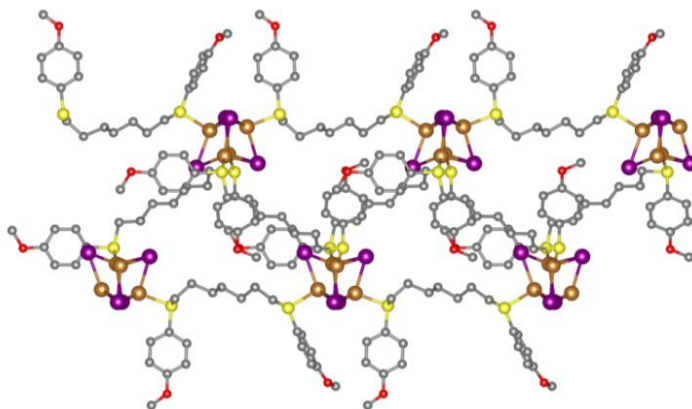


Figure 9. Calculated structure of **CP7** ($1\text{D}-[\text{Cu}_4\text{I}_4(\text{L7})_2]_n$). The H-atoms are not shown for clarity. Color code: brown (Cu), purple (I), yellow (S), red (O), grey (C).

X-ray structure of **CP8** ($3\text{D}-[\text{Cu}_4\text{I}_4(\text{L8})_2]_n$). The crystal structure of **CP8**, which was obtained by treatment of CuI with bis(4-methoxyphenylthio)octane **L8** in MeCN solution, consists of 3D-network with a Cu_4I_4 closed cubane as *globular* SBU (Figure 10, two views of the crystal packings

are provided in Figure S15). The choice of the solvent can have in certain cases a dramatic impact on the resulting network architecture as exemplified for **CP3** and **CP3'**. We have also recently demonstrated that outcome of the reaction of CuI with **L4** depends crucially on the choice of acetonitrile vs propionitrile.³⁸ Therefore, we also performed the reaction with EtCN instead MeCN as solvent. However, in the case of **L8**, no impact on the architecture was observed; in both cases the material crystallizes in the tetragonal space group $I41/a$.

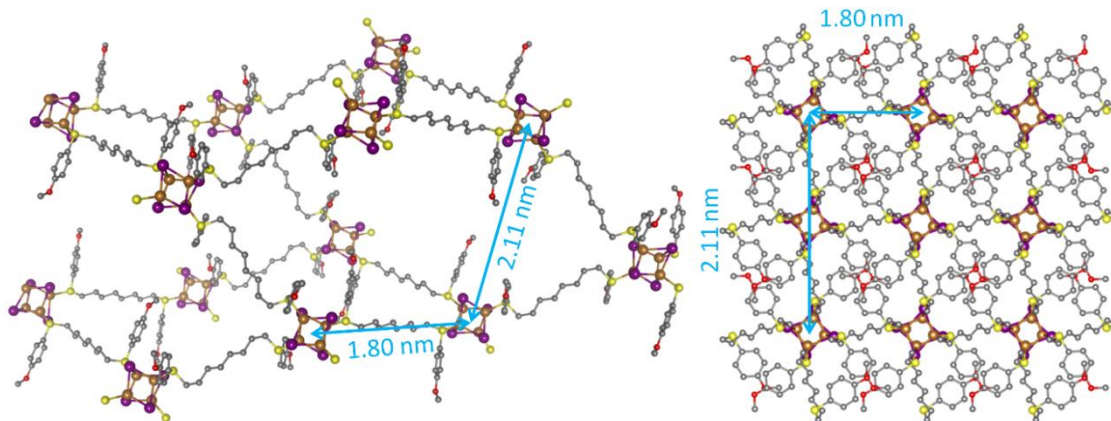


Figure 10. X-ray structure of **CP8** ($3D-[Cu_4I_4(L8)_2]_n$). Side (left) and top (right) views of the crystal packing. The H-atoms are not shown for clarity. Color code: brown (Cu), purple (I), yellow (S), red (O), grey (C).

This result is consistent with the fact that CPs built with (aryl)S(CH₂)₈S(aryl) CPs (aryl = 4-C₆H₄R; R = H, Me, ^tBu) ligands and CuI generate systematically *globular* SBUs, namely closed cubane and fused closed dicubane.^{41,45} However, the dimensionality remains unpredictable, since with PhS(CH₂)₈SPh and *p*-TolS(CH₂)₈STol-*p*, 1D and 2D networks are respectively generated. The 3D-dimensionality in Cu₄I₄-containing chalcogenide networks is not statistically frequent (10%).³⁶ The other 3D-CPs in this series is **CP4**, [(Cu₈I₈)(**L4**)₂]_n, where **L4** bears a (CH₂)₄ chain.³⁸ The link between **CP4** and **CP8** is noteworthy since both share similarities. Both CPs are 3D, use a *globular* SBU, and the (CH₂)_m chains exhibit *m* = 8 in **CP8** and *m* = 4 in **CP4**, stressing the fact that one is a factor of the other. Due to the nanometric separations between the neighbored Cu₄I₄ clusters (centroid-to-centroid distances of ~ 2 nm, Figure 12) caused by the long and flexible (CH₂)₈ spacer, the crystal packing suggests the presence of large voids. But again, the calculated filled and void spaces fall with the range observed for the CPs studied herein meaning that **CP8** is not porous (Table S4). Moreover, the temperature dependence of the unit cell parameters

(Table S3; Figure S16) recorded at six different temperatures (100, 150, 173, 200, 250 and 293 K) does not show evidence for a phase transition occurring in this 193 K interval. The Cu...Cu separations increase by $\sim 0.03\text{-}0.04$ Å over this temperature range.

Photophysical properties. All CPs are white but intense yellow emissions were observed with naked eyes for **CP3**, **CP5** and **CP7** samples when subjected to UV light at 298 K (Figure S17). **CP2**, **CP6** and **CP8** exhibit faint blue luminescence (Figure S17). Prior all measurements of their photophysical properties (Table 3), each powder samples was checked for crystalline purity by comparing the PXRD patterns with the calculated ones issued from the crystal data (Figure S18). The absorption and excitation spectra exhibit signal below 350 nm (Figures S19-S25). The emission bands are found to be structureless and their maxima are found in the usual range for thioether/copper iodide species (500-750 nm).³⁶ This band is assigned to cluster-centered excited states (³CC*) for Cu₄I₄-containing CPs (**CP1**, **CP3**, **CP5**, **CP7** and **CP8**). A weak high energy emission band in the 400-500 nm range is observed for **CP8** at 77 K ($\lambda_{\text{emi}} \sim 440$ nm, Figure S25). Such band high energy band for cubane-type clusters is generally associated with a metal/halide-to-ligand charge transfer excited state, ³M/XLCT*,³⁶ but was not investigated further. Moreover, several species copper iodide clusters exhibit emission thermochromism. One relevant example is the cubane-containing species (CuI)₄(MeCN)₄L (L = dibenzo-18-crown-6), which exhibits a yellow emission at 298 K and pink luminescence at 77 K.⁴⁶ Several thioether/copper iodide CPs and discrete complexes are also known for emission thermochromism.⁴⁹⁻⁵³ Except for the previously reported **CP4**, no emission thermochromism was detected in this series.³⁸

Table 3. Photophysical data of the CPs.

CP	$\lambda_{\text{emi max}}$ (nm)		τ_e (μs) ^a		Φ_e ^b
	77 K	298 K	77 K	298 K	298 K
CP1 ⁴⁰	548	550	24.2	10.3	— ^b
CP2	587	680	15.0	6.0	< 0.001
CP3	600	582	2.5, 10.4, 26.6	0.45, 6.5, 15.2	0.27
CP4 ³⁸	420, 770	740	— ^{c,d}	0.28, 1.8	< 0.001
CP5	564	564	15.14	7.5	0.24
CP6	611	531	6.29	1.46	0.09
CP7	554	574	5.99	5.03	0.23
CP8	554	515	13.4	0.60	0.11

^aThe uncertainty is $\pm 10\%$. ^bNot measured in this study. ^cToo weak to be measured (770 nm). ^dDecay is shorter than the FWHM of the excitation pulse (100 ps; this 440 nm band is due to a ligand-localized triplet excited state, $^3\pi^*$).³⁸

The emission quantum yield (Φ_e) measurements (at 298 K) allow for the division into two categories: strong yellow emission; **CP1**, **CP3**, **CP5**, and **CP7** ($\Phi_e > 0.23$), and weak blueish luminescence; **CP2**, **CP4**, **CP6** and **CP8** ($\Phi_e < 0.11$), with the latter group being less intense (note that this latter 0.11 value is associated with a Cu_4I_4 chromophore, which is usually strongly emissive). The quantum yield of **CP1** is not known but it is reported to be strongly emissive.⁴⁰ It is quite interesting to note that the color of the glow and the emission quantum yield are function of the odd or even number of methylene groups in the chain ($m = \text{odd number}$, yellow glow and $\Phi_e > 0.23$; $m = \text{even number}$, weak blueish emission and $\Phi_e < 0.11$).

The emission lifetimes are expectedly in the μs time scale (from 0.6 to 27 μs), and the decays are either mono- or poly-exponential (the decays and their analyses are provided in Figures S26-S31). The variability of emission lifetimes in the solid state are sometime function of the morphology. In recent studies, temperature, thermal annealing, type of stacking, and effect of grinding were parameters that influenced the number of components to fit an emission decay and the size of the emission lifetimes of inorganic complexes in the solid state.^{54,55} Thermal annealing and grinding have for effect to decrease the emission lifetimes. **CP3** ($1\text{D-}[\{\text{Cu}_4\text{I}_4(\text{L3})_2\}_{3.5}\cdot\text{Cu}_4\text{I}_4(\text{MeCN})_4\cdot 4\text{MeCN}]_n$) is susceptible to undergo a mechano-induced phase change upon grinding and was selected for testing along with **CP5** to assess whether grinding the solid affects the emission decays. The results are placed in Table 4 (the decays are placed in Figures S27 and S28). No mechano-thermochromism was detected, and the emission lifetimes decreased upon grinding the samples. The mechanic stress has for effect to create physical tension and decrease some interatomic distances, thus increasing non-radiative processes due to intermolecular collisions. All in all, emission lifetimes recorded in the solid state may vary from one sample to another depending on the way they were previously treated.

Table 4. Effect of grinding **CP3** and **CP5** on their emission decays.

CP	τ_e (μs) $\{B\}^{a,b}$			χ^2
CP3	0.45 {0.0202}	6.5 {0.0070}	15.2 {0.0138}	1.02
Grinded CP3	0.32 {0.0051}	2.3 {0.0037}	7.7 {0.0020}	0.99
CP5	7.5 {0.0048}	—	—	0.98

Grinded CP5	5.7 {0.0055}	—	—	1.09
--------------------	--------------	---	---	------

^aThe uncertainty is $\pm 10\%$. ^b $I_e(t) = B_1 \exp(-t/\tau_1) + B_2 \exp(-t/\tau_2) + B_3 \exp(-t/\tau_3) + \dots$

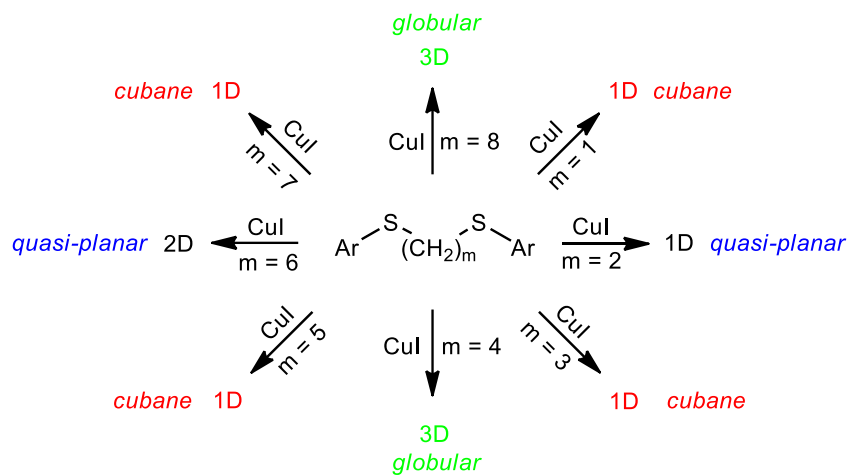
Final comments. One of the largest difficulties in the design of CPs is the predictability of the resulting SBU motif and the CP dimensionality. For CuX salts, the rhomboid motif ($\text{Cu}_2(\mu\text{-X})_2$) dominates overwhelmingly the resulting SBU motif ($\text{X} = \text{Cl}, \text{Br}$), and for $\text{X} = \text{Br}$, weak emission of the resulting CP is often noted.³⁶ Occasionally, the ligand/CuX ratio ($\text{X} = \text{I}$), namely 2:1 and 1:1, directs the formation of respectively *quasi-planar* (mostly rhomboid) or a *globular* SBUs,^{40,56–58} where the *globular* ones exhibit the most intense emission. These two information (*i.e.* nature of X and ligand/CuI ratio of the reaction) are useful to make a preliminary assessment of the expected SBU type and thus on its foreseen emission characteristics. However exceptions may exist due to the variation in steric constraint around the S-atom and the nature of the chain in ditopic ligands, which dictate the bite distance and rigidity.³⁶ The main conclusion of this review is that the $(\text{CuI})_n$ SBU adapts its shape and size according to its environment imposed by its ligand.

The simplest flexible chain is the polymethylene for $(\text{aryl})\text{S}(\text{CH}_2)_m\text{S}(\text{aryl})$ ($\text{aryl} = 4\text{-C}_6\text{H}_4\text{R}$; $\text{R} = \text{H}, \text{Me}, \text{tBu}$). To the best of knowledge, a systematic investigation where a complete set of $\text{S}(\text{CH}_2)_m\text{S}$ chains ($1 \leq m \leq 8$) are studied, appears inexistent. In this work, $1 \leq m \leq 8$, thus keeping at play only one variable. A trend between odd and even number of m has been noticed about the luminescence color and intensity. Table 5 and Figure 11 (top) summarize several of these depicted characteristics. From Figure 11, symmetric features are obvious, notably for $m = 1, 3, 5, 7$.

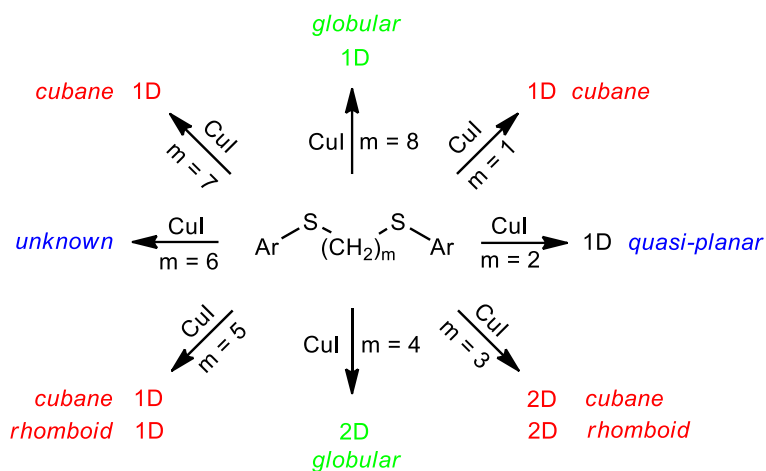
Table 5. Comparison of the SBU properties and the CP emission traits.^a

CP	$(\text{CH}_2)_m$	ref.	SBU motif	SBU type	xD-CP	relative emission intensity [Φ_e]
CP1 ⁴⁰	$m = 1$	^{38,39}	Cu_4I_4 cubane	globular	1D	Strongly [-]
CP2	$m = 2$	<i>tw</i>	$(\text{Cu}_2\text{I}_2)_n$ 1D-staircase ribbon	quasi-planar	1D	Weakly [< 0.001]
CP3	$m = 3$	<i>tw</i>	Cu_4I_4 cubane	globular	1D	Strongly [0.27]
CP4 ³⁸	$m = 4$	⁴⁰	Cu_8I_8 1D-poly(truncated rhombic dodecahedron)	globular	3D	weakly (near-IR) [< 0.001]
CP5	$m = 5$	<i>tw</i>	Cu_4I_4 cubane	globular	1D	Strongly [0.24]
CP6	$m = 6$	<i>tw</i>	$(\text{Cu}_2\text{I}_2)_n$ 1D-accordion ribbon	quasi-planar	2D	Medium [0.09]
CP7	$m = 7$	<i>tw</i>	Cu_4I_4 cubane	globular	1D	Strongly [0.23]
CP8	$m = 8$	<i>tw</i>	Cu_4I_4 cubane	globular	3D	Medium [0.11]

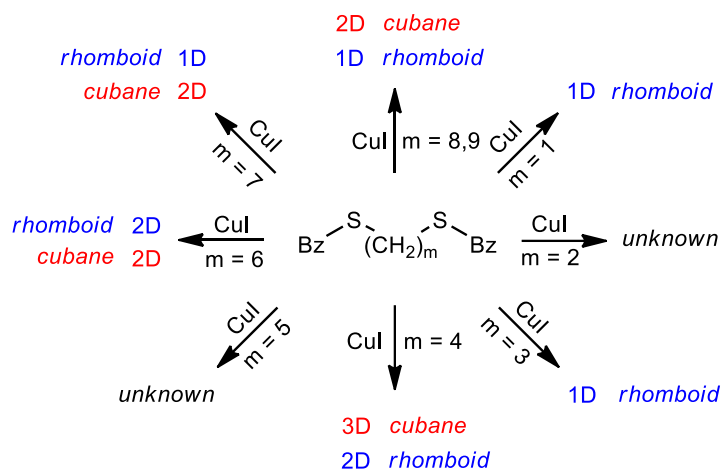
^a*tw* = this work.



4-MeOC₆H₄MeS(CH₂)_mSC₆H₄OMe/CuI-containing CPs



PhS(CH₂)_mSPh/CuI-containing CPs



BzS(CH₂)_mSBz/CuI-containing CPs

Figure 11. Comparison of some structural features, namely nature of the SBU and CP dimensionality for Ar = 4-C₆H₄OMe (top; note that for the case when $m = 3$ using EtCN as

solvent, the 1D-CP **CP3'** is generated and the rhomboid SBU is formed), for Ar = Ph (middle; this information is extracted from references 22, 27, 29, and 36. Note that the quasi-planar SBU is a 0D-rhomboid, and that the presence of cubane and rhomboid for a same reaction is due to the ligand/CuI stoichiometric ratio employed) and for BzS(CH₂)_mSBz/CuI-containing CPs (bottom; red = closed cubane; blue = rhomboid. Note that the case where $m = 9$ is also available. This information is extracted from reference ⁵⁸). Solvent = MeCN.

Furthermore, it is noteworthy that 1D-SBU are formed when $m = 2, 4,$ and $6,$ and one wonder whether this situation is due to a coincidence. To address this point, the case where X = H is examined where only the case for $m = 6$ is not available (Figure 11, middle). The similarity in symmetry with that of Figure 11 is striking (not identical, particularly for the CP dimensionality). However, no 1D-SBU is formed meaning that the formation of 1D-SBUs in the X = OMe series is a coincidence and specific to the substituent. Such effect has been observed before.⁵⁹

Finally, the replacement of an aryl group by a benzyl one reduces the steric hindrance around the S-donor (Figure 11, bottom).⁵⁸ The consequence is that both rhomboid and cubane motifs are readily formed and readily directed from the ligand/CuI ratio. Indeed, five of the seven available m data lead to both cubane and rhomboid motifs, and mostly 1D- and 2D-CPs have been isolated. The conclusion is that the cubane and rhomboid motifs, and the 1D- and 2D-CPs are the most stable structures when steric constraint around the S-atom is minimum in flexible bidentate ligands. Consequently, the aryl group (RC₆H₄-) imposes some steric hindrance and in conjunction with the odd and even number of methylene units in the (CH₂)_m chain, symmetry in the outcome of the resulting SBU motifs is noted (Figure 11). Such analysis and observation are unprecedented.

By comparison, the Ph₂P(CH₂)_mPPh₂ ligands ($m = 1-6$) do not form CPs when reacted with CuI. Instead, 0D-Ph₂P(CH₂)_mPPh₂/CuI complexes bearing various (CuI)_n units ($m = 1, 2$ (rhomboid), 3 (cyclic), 4 (staircase), 6 (cubane with two flanking CuI units) have been isolated.⁶⁰⁻⁶⁵ It is noteworthy that only the latter case, Cu₆I₆, has a *globular* shape whereas all other ones are *quasi-planar*. The reason for the absence of CPs and the dominant *quasi-planar* shape for the SBUs stems from the imposing steric constraint of the PPh₂ groups around the P-atom. To the best of our knowledge, only one CPs has been reported for a diphosphine/CuI system. In this case, the ligand is rigid Ph₂P-C₆H₄-C₆H₄-PPh₂ but the claim was not supported by a X-ray structure.²⁰

Conclusion

There is a clear effect of the chain length on the structural features of the SBU and in a lesser extent on the CP dimensionality in ditopic thioether ligand reacting with CuI. This observation is to the best of our knowledge, unprecedented. For ligands with lesser encumbered S-atoms, the outcome becomes ligand/CuI ratio-dependent. These observation makes the prediction of the outcome of a reaction between the bidentate $\text{ArS}(\text{CH}_2)_m\text{SAr}$ ligand with CuI less obscure. The next step is to generalize this trend where the R group in the 4- RC_6H_4 unit is also systematically varied (R = H, Me, OMe, F, Cl, Br, ^tBu).

No unexpected, new, and/or significant hazards or risks are associated with the reported work.

ASSOCIATED CONTENT

Supporting Information. Experimental section, IR and Raman spectra of **CP2,3,5,6,7,8**, X-ray data and selected views of crystal packings of **CP2,3',6,8**, temperature dependence of unit cell parameters of **CP2** and **CP8**, powder X-ray diffraction patterns of **CP2,3,5,6,8**, TGA traces of **CP2,3,3',5-8**, images of the CPs under day and UV-light, absorption, emission and excitation spectra at 298 and 77K, and emission decays of **CP3,5,7,8**. (PDF)

Accession Codes. CCDC 2164870-2164877, 2164896, 2164898, 2164904, 2164946, 2164948, 2164951 contain the supplementary crystallographic data for this paper. These data can be obtained free of charge via www.ccdc.cam.ac.uk/data_request/cif, or by emailing data_request@ccdc.cam.ac.uk, or by contacting The Cambridge Crystallographic Data Centre, 12 Union Road, Cambridge CB2 1EZ, UK; fax: +44 1223 336033.

AUTHOR INFORMATION

Corresponding Author

*E-mail: Adrien.Schlachter@USherbrooke.ca (A.S.)

*E-mail: Pierre.Harvey@USherbrooke.ca (P.D.H.)

*E-mail: Michael.Knorr@univ-fcomte.fr (M.K.).

Author Contributions

Conceptualization, A.S., M.K. and P.D.H.; methodology, A.S.; software, A.S.; validation, A.S., M.K., and P.D.H.; formal analysis, A.S.; investigation, A.S. D.F.; resources, P.D.H., M.K., and C.S.; data curation, A.S.; writing—original draft preparation, P.D.H.; writing—review and editing, A.S., M.K., and P.D.H.; visualization, A.S.; supervision, P.D.H., M.K.; project administration, A.S.; funding acquisition, P.D.H. and M.K. All authors have read and agreed to the published version of the manuscript.

Notes

The authors declare no competing financial interest.

ACKNOWLEDGMENT

This work was supported by the Natural Sciences and Engineering Research Council of Canada (NSERC). M.K. and C.S. thank the CNRS and the DFG for financial support. Mr G. Marineau Plante (Ms.C.) is thanked for some complementary investigations.

REFERENCES

- (1) Hardt, H. D.; Stoll, H. J. Über Das Fluoreszenzthermochrome Acetonitrilo-Kupferjodid Mit Dibenzo-18-Krone-6. *ZAAC - J. Inorg. Gen. Chem.* **1978**, *442* (1), 221–224. <https://doi.org/10.1002/zaac.19784420129>.
- (2) Hardt, H. D.; Stoll, H. J. Fluoreszenzeigenschaften der beiden Modifikationen des (4-Phenylpyridintriphenylphosphan)Kupfer(I)-Iodids. *Naturwissenschaften* **1980**, *67* (12), 606–607. <https://doi.org/10.1007/BF00396547>.
- (3) Hardt, H. D.; Stoll, H. -J. Wirkung von Substituenten und Anionen auf die Fluoreszenzeigenschaften gemischtligandiger (Amin-triphenylphosphan)Kupfer(I)-Halogenide. *Z. Anorg. All. Chem.* **1981**, *480* (9), 199–204. <https://doi.org/10.1002/zaac.19814800926>.
- (4) Hardt, H. D.; Stoll, H. -J. Neue Ergebnisse zu den Fluoreszenzeigenschaften von Sesqui-, Bis- und Tris(Triphenylphosphan)Kupfer(I)-Halogeniden. *Z. Anorg. All. Chem.* **1981**, *480* (9), 193–198. <https://doi.org/10.1002/zaac.19814800925>.

- (5) Ford, P. C.; Cariati, E.; Bourassa, J. Photoluminescence Properties of Multinuclear Copper(I) Compounds. *Chem. Rev.* **1999**, *99* (12), 3625–3647. <https://doi.org/10.1021/cr960109i>.
- (6) Conesa-Egea, J.; Zamora, F.; Amo-Ochoa, P. Perspectives of the Smart Cu-Iodine Coordination Polymers: A Portage to the World of New Nanomaterials and Composites. *Coord. Chem. Rev.* **2019**, *381*, 65–78. <https://doi.org/10.1016/j.ccr.2018.11.008>.
- (7) Kobayashi, A.; Kato, M. Stimuli-Responsive Luminescent Copper(I) Complexes for Intelligent Emissive Devices. *Chem. Lett.* **2017**, *46* (2), 154–162. <https://doi.org/10.1246/cl.160794>.
- (8) Liu, W.; Fang, Y.; Li, J. Copper Iodide Based Hybrid Phosphors for Energy-Efficient General Lighting Technologies. *Adv. Funct. Mater.* **2018**, *28* (8), 1705593. <https://doi.org/10.1002/adfm.201705593>.
- (9) Ardizzoia, G. A.; Brenna, S. Hydroxo-Bridged Copper(II) Cubane Complexes. *Coord. Chem. Rev.* **2016**, *311*, 53–74. <https://doi.org/10.1016/j.ccr.2015.11.013>.
- (10) Chakraborty, G.; Park, I. H.; Medishetty, R.; Vittal, J. J. Two-Dimensional Metal-Organic Framework Materials: Synthesis, Structures, Properties and Applications. *Chem. Rev.* **2021**, *121* (7), 3751–3891. <https://doi.org/10.1021/acs.chemrev.0c01049>.
- (11) Troyano, J.; Zamora, F.; Delgado, S. Copper(i)-Iodide Cluster Structures as Functional and Processable Platform Materials. *Chem. Soc. Rev.* **2021**, *50* (7), 4606–4628. <https://doi.org/10.1039/d0cs01470b>.
- (12) Perruchas, S. Molecular Copper Iodide Clusters: A Distinguishing Family of Mechanochromic Luminescent Compounds. *Dalton Trans.* **2021**, *50* (35), 12031–12044. <https://doi.org/10.1039/d1dt01827b>.
- (13) Gschwind, F.; Sereda, O.; Fromm, K. M. Multitopic Ligand Design: A Concept for Single-Source Precursors. *Inorg. Chem.* **2009**, *48* (22), 10535–10547. <https://doi.org/10.1021/ic9009064>.
- (14) Peng, R.; Li, M.; Li, D. Copper(I) Halides: A Versatile Family in Coordination Chemistry

- and Crystal Engineering. *Coord. Chem. Rev.* **2010**, *254* (1–2), 1–18. <https://doi.org/10.1016/j.ccr.2009.10.003>.
- (15) Fang, Y.; Liu, W.; Teat, S. J.; Dey, G.; Shen, Z.; An, L.; Yu, D.; Wang, L.; O'Carroll, D. M.; Li, J. A Systematic Approach to Achieving High Performance Hybrid Lighting Phosphors with Excellent Thermal- and Photostability. *Adv. Funct. Mater.* **2017**, *27* (3), 1603444. <https://doi.org/10.1002/adfm.201603444>.
- (16) Tan, Y. X.; He, Y. P.; Zhang, J. Cluster-Organic Framework Materials as Heterogeneous Catalysts for High Efficient Addition Reaction of Diethylzinc to Aromatic Aldehydes. *Chem. Mater.* **2012**, *24* (24), 4711–4716. <https://doi.org/10.1021/cm302953x>.
- (17) Fang, W. H.; Wang, J. F.; Zhang, L.; Zhang, J. Titanium-Oxo Cluster Based Precise Assembly for Multidimensional Materials. *Chem. Mater.* **2017**, *29* (7), 2681–2684. <https://doi.org/10.1021/acs.chemmater.7b00324>.
- (18) Xie, M.; Han, C.; Zhang, J.; Xie, G.; Xu, H. White Electroluminescent Phosphine-Chelated Copper Iodide Nanoclusters. *Chem. Mater.* **2017**, *29* (16), 6606–6610. <https://doi.org/10.1021/acs.chemmater.7b01443>.
- (19) Shan, X. C.; Jiang, F. L.; Chen, L.; Wu, M. Y.; Pan, J.; Wan, X. Y.; Hong, M. C. Using Cuprophilicity as a Multi-Responsive Chromophore Switching Color in Response to Temperature, Mechanical Force and Solvent Vapors. *J. Mater. Chem. C* **2013**, *1* (28), 4339–4349. <https://doi.org/10.1039/c3tc30482e>.
- (20) Benito, Q.; Desboeufs, N.; Fargues, A.; Garcia, A.; Massuyeau, F.; Martineau-Corcus, C.; Devic, T.; Perruchas, S. A Photoactive Copper Iodide Phosphine-Based Coordination Polymer. *New J. Chem.* **2020**, *44* (45), 19850–19857. <https://doi.org/10.1039/d0nj04486e>.
- (21) Jai, Y. L.; So, Y. L.; Sim, W.; Park, K. M.; Kim, J.; Shim, S. L. Temperature-Dependent 3-D CuI Coordination Polymers of Calix[4]-Bis-Dithiacrown: Crystal-to-Crystal Transformation and Photoluminescence Change on Coordinated Solvent Removal. *J. Am. Chem. Soc.* **2008**, *130* (22), 6902–6903. <https://doi.org/10.1021/ja8008693>.
- (22) Zhao, S.; Wang, L.; Liu, Y.; Chen, L.; Xie, Z. Stereochemically Dependent Synthesis of

- Two Cu(I) Cluster-Based Coordination Polymers with Thermochromic Luminescence. *Inorg. Chem.* **2017**, *56* (22), 13975–13981. <https://doi.org/10.1021/acs.inorgchem.7b02123>.
- (23) Yang, K.; Li, S. L.; Zhang, F. Q.; Zhang, X. M. Simultaneous Luminescent Thermochromism, Vapochromism, Solvatochromism, and Mechanochromism in a C₃-Symmetric Cubane [Cu₄I₄P₄] Cluster without Cu-Cu Interaction. *Inorg. Chem.* **2016**, *55* (15), 7323–7325. <https://doi.org/10.1021/acs.inorgchem.6b00922>.
- (24) Yin, S.-Y.; Wang, Z.; Liu, Z.-M.; Yu, H.-J.; Zhang, J.-H.; Wang, Y.; Mao, R.; Pan, M.; Su, C.-Y. Multiresponsive UV-One-Photon Absorption, Near-Infrared-Two-Photon Absorption, and X/γ-Photoelectric Absorption Luminescence in One [Cu₄I₄] Compound. *Inorg. Chem.* **2019**, *58* (16), 10736–10742. <https://doi.org/10.1021/ACS.INORGCHEM.9B00876>.
- (25) Fu, Z.; Lin, J.; Wang, L.; Li, C.; Yan, W.; Wu, T. Cuprous Iodide Pseudopolymorphs Based on Imidazole Ligand and Their Luminescence Thermochromism. *Cryst. Growth Des.* **2016**, *16* (4), 2322–2327. <https://doi.org/10.1021/acs.cgd.6b00114>.
- (26) Song, Y.; Fan, R.; Wang, P.; Wang, X.; Gao, S.; Du, X.; Yang, Y.; Luan, T. Copper(I)-Iodide Based Coordination Polymers: Bifunctional Properties Related to Thermochromism and PMMA-Doped Polymer Film Materials. *J. Mater. Chem. C* **2015**, *3* (24), 6249–6259. <https://doi.org/10.1039/c5tc01273b>.
- (27) Park, H.; Kwon, E.; Chiang, H.; Im, H.; Lee, K. Y.; Kim, J.; Kim, T. H. Reversible Crystal Transformations and Luminescence Vapochromism by Fast Guest Exchange in Cu(I) Coordination Polymers. *Inorg. Chem.* **2017**, *56* (14), 8287–8294. <https://doi.org/10.1021/acs.inorgchem.7b00951>.
- (28) Kwon, E.; Kim, J.; Lee, K. Y.; Kim, T. H. Non-Phase-Transition Luminescence Mechanochromism of a Copper(I) Coordination Polymer. *Inorg. Chem.* **2017**, *56* (2), 943–949. <https://doi.org/10.1021/acs.inorgchem.6b02571>.
- (29) Jai, Y. L.; Hyun, J. K.; Jong, H. J.; Sim, W.; Shim, S. L. Networking of Calixcrowns: From Heteronuclear Endo/Exocyclic Coordination Polymers to A Photoluminescence

- Switch. *J. Am. Chem. Soc.* **2008**, *130* (42), 13838–13839. <https://doi.org/10.1021/ja805337n>.
- (30) Shen, W.; El Sayed Moussa, M.; Yao, Y.; Lescop, C. Supramolecular Metallacycles with a ‘Pseudo Double-Paracyclophane’ Structure Based on Flexible π -Conjugated Linkers. *Chem. Commun.* **2015**, *51* (58), 11560–11563. <https://doi.org/10.1039/C5CC03778F>.
- (31) Elsayed Moussa, M.; Evariste, S.; Krämer, B.; Réau, R.; Scheer, M.; Lescop, C. Can Coordination-Driven Supramolecular Self-Assembly Reactions Be Conducted from Fully Aliphatic Linkers? *Angew. Chem. Int. Ed.* **2018**, *57* (3), 795–799. <https://doi.org/10.1002/anie.201709119>.
- (32) Lescop, C. Coordination-Driven Supramolecular Synthesis Based on Bimetallic Cu(I) Precursors: Adaptive Behavior and Luminescence. *Chem. Rec.* **2021**, *21* (3), 544–557. <https://doi.org/10.1002/tcr.202000144>.
- (33) Peresyphkina, E.; Grill, K.; Hiltl, B.; Virovets, A. V.; Kremer, W.; Hilgert, J.; Tremel, W.; Scheer, M. Three-Component Self-Assembly Changes Its Course: A Leap from Simple Polymers to 3D Networks of Spherical Host–Guest Assemblies. *Angew. Chem. Int. Ed.* **2021**, *60* (21), 12132–12142. <https://doi.org/10.1002/anie.202103178>.
- (34) Streitberger, M.; Schmied, A.; Hey-Hawkins, E. Selective Formation of Gold(I) Bis-Phospholane Macrocycles, Polymeric Chains, and Nanotubes. *Inorg. Chem.* **2014**, *53* (13), 6794–6804. <https://doi.org/10.1021/ic5006055>.
- (35) Boar, P.; Streitberger, M.; Lönnecke, P.; Hey-Hawkins, E. Copper(I) Complexes of a Flexible Bis-Phospholane Ligand: Route to Paddle-Wheel- and Box-Type Macrocycles. *Inorg. Chem.* **2017**, *56* (12), 7285–7291. <https://doi.org/10.1021/acs.inorgchem.7b01046>.
- (36) Schlachter, A.; Tanner, K.; Harvey, P. D. Copper Halide-Chalcogenoether and -Chalcogenone Networks: Chain and Cluster Motifs, Polymer Dimensionality and Photophysical Properties. *Coord. Chem. Rev.* **2021**, *448*, 214176. <https://doi.org/10.1016/j.ccr.2021.214176>.
- (37) Schlachter, A.; Harvey, P. D. Properties and Applications of Copper Halide-

- Chalcogenoether and -Chalcogenone Networks and Functional Materials. *J. Mater. Chem. C* **2021**, *9* (21), 6648–6685. <https://doi.org/10.1039/d1tc00585e>.
- (38) Schlachter, A.; Tanner, K.; Scheel, R.; Karsenti, P. L.; Strohmamm, C.; Knorr, M.; Harvey, P. D. A Fused Poly(Truncated Rhombic Dodecahedron)-Containing 3D Coordination Polymer: A Multifunctional Material with Exceptional Properties. *Inorg. Chem.* **2021**, *60* (17), 13528–13538. <https://doi.org/10.1021/acs.inorgchem.1c01856>.
- (39) Peindy, H. N.; Guyon, F.; Khatyr, A.; Knorr, M.; Strohmamm, C. Construction of 1D and 2D Copper(I) Coordination Polymers Assembled by PhS(CH₂)_nNSPh (n = 1, 2) Dithioether Ligands: Surprising Effect of the Spacer Length on the Dimensionality, Cluster Nuclearity and the Fluorescence Properties of the Metal-Organic Frame. *Eur. J. Inorg. Chem.* **2007**, *2007* (13), 1823–1828. <https://doi.org/10.1002/ejic.200600954>.
- (40) Knorr, M.; Khatyr, A.; Dini Aleo, A.; El Yaagoubi, A.; Strohmamm, C.; Kubicki, M. M.; Rousselin, Y.; Aly, S. M.; Fortin, D.; Lapprand, A.; Harvey, P. D. Copper(I) Halides (X = Br, I) Coordinated to Bis(Arylthio)Methane Ligands: Aryl Substitution and Halide Effects on the Dimensionality, Cluster Size, and Luminescence Properties of the Coordination Polymers. *Cryst. Growth Des.* **2014**, *14* (11), 5373–5387. <https://doi.org/10.1021/cg500905z>.
- (41) Bonnot, A.; Juvenal, F.; Lapprand, A.; Fortin, D.; Knorr, M.; Harvey, P. D. Can a Highly Flexible Copper(i) Cluster-Containing 1D and 2D Coordination Polymers Exhibit MOF-like Properties? *Dalton Trans.* **2016**, *45* (28), 11413–11421. <https://doi.org/10.1039/c6dt01375a>.
- (42) Raghuvanshi, A.; Knorr, M.; Knauer, L.; Strohmamm, C.; Boullanger, S.; Moutarlier, V.; Viau, L. 1,3-Dithianes as Assembling Ligands for the Construction of Copper(I) Coordination Polymers. Investigation of the Impact of the RC(H)S₂C₃H₆ Substituent and Reaction Conditions on the Architecture of the 0D-3D Networks. *Inorg. Chem.* **2019**, *58* (9), 5753–5775. <https://doi.org/10.1021/acs.inorgchem.9b00114>.
- (43) Knorr, M.; Guyon, F. Luminescent Oligomeric and Polymeric Copper Coordination Compounds Assembled by Thioether Ligands. In *Macromolecules Containing Metal and*

- Metal-Like Elements*; Abd-El Aziz, A. S., Carraher, C. E., Harvey, P. D., Pittman, C. U., Zeldin, M., Eds.; John Wiley & Sons, Inc.: Hoboken, NJ, USA, 2010; Vol. 10, pp 89–158. <https://doi.org/10.1002/9780470604090.ch3>.
- (44) Saha, S.; Biswas, K.; Ghosh, P.; Basu, B. New 1,2-Dithioether Based 2D Copper(I) Coordination Polymer: From Synthesis to Catalytic Application in A³-Coupling Reaction. *J. Coord. Chem.* **2019**, *72* (11), 1810–1819. <https://doi.org/10.1080/00958972.2019.1627339>.
- (45) Harvey, P. D.; Bonnot, A.; Lapprand, A.; Strohmam, C.; Knorr, M. Coordination RC₆H₄S(CH₂)₈SC₆H₄R/(CuI)_n Polymers (R (n) = H (4); Me (8)): An Innocent Methyl Group That Makes the Difference. *Macromol. Rapid Commun.* **2015**, *36* (7), 654–659. <https://doi.org/10.1002/marc.201400659>.
- (46) Jasinski, J. P.; Rath, N. P.; Holt, E. M. Structural Comparison of (CuI)CH₃CN₄·dibenzo-18-Crown-6 (I) and (CuI)CH₃CN)_x (II) Fluorescent Copper(I) Materials. *Inorg. Chim. Acta* **1985**, *97* (1), 91–97. [https://doi.org/10.1016/S0020-1693\(00\)87995-5](https://doi.org/10.1016/S0020-1693(00)87995-5).
- (47) Knorr, M.; Guyon, F.; Khatyr, A.; Strohmam, C.; Allain, M.; Aly, S. M.; Lapprand, A.; Fortin, D.; Harvey, P. D. Construction of (CuX)_{2n} Cluster-Containing (X = Br, I; N = 1, 2) Coordination Polymers Assembled by Dithioethers ArS(CH₂)MSAr (Ar = Ph, p-Tol; M = 3, 5): Effect of the Spacer Length, Aryl Group, and Metal-to-Ligand Ratio on the Dimensionality, Cluster . *Inorg. Chem.* **2012**, *51* (18), 9917–9934. <https://doi.org/10.1021/ic301385u>.
- (48) Saha, S.; Biswas, K.; Basu, B. 1-D Copper(I) Coordination Polymer Based on Bidentate 1,3-Dithioether Ligand: Novel Catalyst for Azide-Alkyne-Cycloaddition (AAC) Reaction. *Tetrahedron Lett.* **2018**, *59* (26), 2541–2545. <https://doi.org/10.1016/j.tetlet.2018.05.040>.
- (49) Henline, K. M.; Wang, C.; Pike, R. D.; Ahern, J. C.; Sousa, B.; Patterson, H. H.; Kerr, A. T.; Cahill, C. L. Structure, Dynamics, and Photophysics in the Copper(I) Iodide-Tetrahydrothiophene System. *Cryst. Growth Des.* **2014**, *14* (3), 1449–1458. <https://doi.org/10.1021/cg500005p>.
- (50) Shan, X. C.; Jiang, F. L.; Yuan, D. Q.; Zhang, H. Bin; Wu, M. Y.; Chen, L.; Wei, J.;

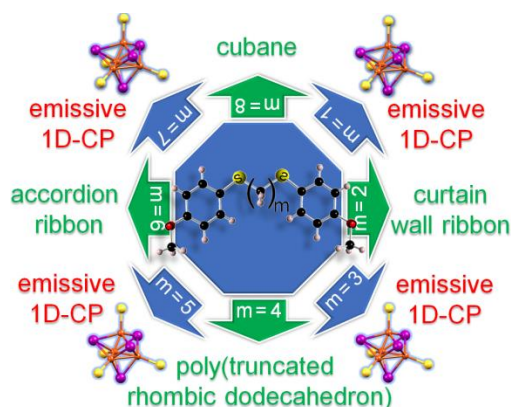
- Zhang, S. Q.; Pan, J.; Hong, M. C. A Multi-Metal-Cluster MOF with Cu₄I₄ and Cu₆S₆ as Functional Groups Exhibiting Dual Emission with Both Thermochromic and near-IR Character. *Chem. Sci.* **2013**, *4* (4), 1484–1489. <https://doi.org/10.1039/c3sc21995j>.
- (51) Knorr, M.; Guyon, F.; Khatyr, A.; Däschlein, C.; Strohmamm, C.; Aly, S. M.; Abd-El-Aziz, A. S.; Fortin, D.; Harvey, P. D. Rigidity effect of the dithioether spacer on the size of the luminescent cluster (Cu₂I₂)_n (n = 2, 3) in their coordination polymers. *Dalton Trans.* **2009**, *0* (6), 948–955. <https://doi.org/10.1039/b816987j>.
- (52) Kim, T. H.; Shin, Y. W.; Jung, J. H.; Kim, J. S.; Kim, J. Crystal-to-Crystal Transformation between Three CuI Coordination Polymers and Structural Evidence for Luminescence Thermochromism. *Angew. Chem. Int. Ed.* **2008**, *47* (4), 685–688. <https://doi.org/10.1002/anie.200704349>.
- (53) Kim, T. H.; Lee, K. Y.; Shin, Y. W.; Moon, S. T.; Park, K. M.; Kim, J. S.; Kang, Y.; Lee, S. S.; Kim, J. New Crystalline Framework Formed from a Podal Ligand with S₂O₂ Donor and CuI: Non-Interpenetrating Square-Grid with Cubane-like Cu₄I₄ Cluster Nodes. *Inorg. Chem. Commun.* **2005**, *8* (1), 27–30. <https://doi.org/10.1016/j.inoche.2004.10.017>.
- (54) Marineau Plante, G.; Fortin, D.; Soldera, A.; Harvey, P. D. Solid-Solid Phase Transitions in [Trans-Pt(PMe₃)₂(C=CC₆H₄R)₂]-Containing Materials (R = O(CH₂)_NH; N = 6, 9, 12, and 15). *Organometallics* **2018**, *37* (15), 2544–2552. <https://doi.org/10.1021/acs.organomet.8b00304>.
- (55) Marineau-Plante, G.; Juvenal, F.; Langlois, A.; Fortin, D.; Soldera, A.; Harvey, P. D. Multiply “Trapped” 3[Trans -Pt(PR₃)₂(CCC₆H₄R)₂]* Conformers in Rigid Media. *Chem. Commun.* **2018**, *54* (8), 976–979. <https://doi.org/10.1039/c7cc09503a>.
- (56) Bonnot, A.; Strohmamm, C.; Knorr, M.; Harvey, P. D. Metal-to-Ligand Ratio Effect on the Size of Copper Iodide and Copper Bromide Clusters in 1,4-Bis(Cyclohexylthio)Butane-Spanned Coordination Polymers. *J. Clust. Sci.* **2014**, *25* (1), 261–275. <https://doi.org/10.1007/s10876-013-0637-5>.
- (57) Schlachter, A.; Viau, L.; Fortin, D.; Knauer, L.; Strohmamm, C.; Knorr, M.; Harvey, P. D.

- Control of Structures and Emission Properties of (CuI)_n 2-Methyldithiane Coordination Polymers. *Inorg. Chem.* **2018**, *57* (21), 13564–13576. <https://doi.org/10.1021/acs.inorgchem.8b02168>.
- (58) Schlachter, A.; Lapprand, A.; Fortin, D.; Strohmman, C.; Harvey, P. D.; Knorr, M. From Short-Bite Ligand Assembled Ribbons to Nanosized Networks in Cu(I) Coordination Polymers Built Upon Bis(Benzylthio)Alkanes (BzS(CH₂)_nSBz; n = 1–9). *Inorg. Chem.* **2020**, *59* (6), 3686–3708. <https://doi.org/10.1021/acs.inorgchem.9b03275>.
- (59) Aly, S. M.; Pam, A.; Khatyr, A.; Knorr, M.; Rousselin, Y.; Kubicki, M. M.; Bauer, J. O.; Strohmman, C.; Harvey, P. D. Cluster-Containing Coordination Polymers Built Upon (Cu₂I₂S₂)_m Units (m = 2, 3) and ArSCH₂C≡CCH₂SAr Ligands: Is the Cluster Size Dependent Upon Steric Hindrance or Ligand Rigidity? *J. Inorg. Organomet. Polym. Mater.* **2014**, *24* (1), 190–200. <https://doi.org/10.1007/s10904-013-9984-9>.
- (60) Zhang, X.; Song, L.; Hong, M.; Shi, H.; Xu, K.; Lin, Q.; Zhao, Y.; Tian, Y.; Sun, J.; Shu, K.; Chai, W. Luminescent Dinuclear Copper(I) Halide Complexes Double Bridged by Diphosphine Ligands: Synthesis, Structure Characterization, Properties and TD-DFT Calculations. *Polyhedron* **2014**, *81*, 687–694. <https://doi.org/10.1016/j.poly.2014.07.034>.
- (61) Effendy; Di Nicola, C.; Fianchini, M.; Pettinari, C.; Skelton, B. W.; Somers, N.; White, A. H. The Structural Definition of Adducts of Stoichiometry MX:Dppx (1:1) M = CuI, AgI, X = Simple Anion, Dppx = Ph₂P(CH₂)_xPPh₂, x = 3–6. *Inorg. Chim. Acta* **2005**, *358* (3), 763–795. <https://doi.org/10.1016/j.ica.2004.09.047>.
- (62) Yang, R.; Lin, K.; Hou, Y.; Wang, D.; Jin, D.; Luo, B.; Chen, L. Synthesis, Structure and Characterization of Binuclear Copper(I) Complexes. *Transit. Met. Chem.* **1997**, *22* (3), 254–258. <https://doi.org/10.1023/A:1018412524042>.
- (63) Fan, L. Q. Crystal Structure of Bis(μ₃-Iodo)-(μ₂-Iodo)-Bis(μ₂-Bis(Diphenylphosphine)Ethane)Tricopper(I) - Dimethylformamide (1:1), Cu₃I₃(C₂₆H₂₄P₂)₂ · C₃H₇NO. *Zeitschrift für Krist. - New Cryst. Struct.* **2011**, *226* (3), 391–393. <https://doi.org/10.1524/ncrs.2011.0176>.
- (64) Benito, Q.; Le Goff, X. F.; Nocton, G.; Fargues, A.; Garcia, A.; Berhault, A.; Kahlal, S.;

Saillard, J. Y.; Martineau, C.; Trébosc, J.; Gacoin, T.; Boilot, J. P.; Perruchas, S. Geometry Flexibility of Copper Iodide Clusters: Variability in Luminescence Thermochemistry. *Inorg. Chem.* **2015**, *54* (9), 4483–4494. <https://doi.org/10.1021/acs.inorgchem.5b00321>.

- (65) Ramaprabhu, S.; Amstutz, N.; Lucken, E. A. C.; Bernardinelli, G. Copper-63,65 Nuclear Quadrupole Resonance of Complexes of Copper(I) Halides with Phosphorus-Containing Ligands. *J. Chem. Soc. Dalton Trans.* **1993**, No. 6, 871–875. <https://doi.org/10.1039/DT9930000871>.

FOR TABLE OF CONTENTS ONLY



The ligands $\text{ArS}(\text{CH}_2)_m\text{SAr}$ ($\text{Ar} = 4\text{-MeOC}_6\text{H}_4$; $1 \leq m \leq 8$) react with CuI to form coordination polymers (CPs) where a direct dependence of $m =$ (odd or even) on the secondary bonding unit motif, CP dimensionality and emission properties, exists.